

A Capacity-Based Search for Energy and Bandwidth Efficient Bit-Interleaved Coded Noncoherent GFSK

Rohit Iyer Seshadri and Matthew C. Valenti

Lane Dept. of Comp. Sci. & Elect. Eng.

West Virginia University

Morgantown, WV 26506-6109

{iyerr, mvalenti}@csee.wvu.edu

***Abstract*—This paper addresses the general problem of finding the combination of code rates and continuous phase modulation (CPM) parameters that have the best energy efficiency for a given spectral efficiency and demodulator complexity. More specifically, bit-interleaved coded modulation (BICM) with noncoherently detected M -ary Gaussian frequency shift keying (GFSK) is considered for the fading channel. First, a sequential, soft-out (SO), soft-decision differential phase detector (SD-DPD) is presented for noncoherent detection of GFSK signals. Next, the capacity for the proposed system under modulation, channel and receiver design constraints is calculated. For a wide range of spectral efficiencies, the optimal (in terms of energy and bandwidth efficiency) combination of GFSK parameters and code rates is found using information theoretic bounds on reliable signaling. Bit error rate simulations using a capacity-approaching binary turbo code reveal that performance within 1 dB of the constrained capacity can be obtained .**

I. INTRODUCTION

Continuous phase modulation (CPM) [1] is a nonlinear modulation scheme well suited for bandwidth constrained applications due to its small spectral side lobes and fast spectral roll-off. Another beneficial feature is that the constant envelope property of CPM permits the use of power efficient nonlinear amplifiers. In order to exploit these properties at improved energy efficiencies, CPM has been combined with channel coding in a substantial body of work.

CPM using a convolutional code was considered in [2], [3]. However, these do not achieve the energy efficiency promised by systems that use capacity-approaching error correcting codes. An alternative approach is to separate a trellis encoder from the CPM modulator by a symbol-wise interleaver, which allows the demodulation process to be decoupled from the

decoding process [4], [5]. Such systems are referred to as *trellis coded CPM* (TCCPM) [6]. While the interleaver precludes true ML joint demodulation and decoding, it can be approximated by using turbo-style processing [6], [7]. If a bit-interleaver is used instead of a symbol-interleaver, the system design, which now boils down to the selection of a good binary code and efficient CPM modulation parameters (modulation index, modulation order and pulse shape), is greatly simplified. The strategy of combining a binary code, bit-interleaver, and M -ary modulator is called *bit-interleaved coded modulation* (BICM) [8], and here we refer to its extension to continuous phase modulation as *BICPM*. Not only is BICPM more convenient to design and implement than TCCPM, results in [6] indicate that BICPM provides higher diversity than TCCPM, which is consistent with results for BICM in general [8].

In communication systems with constraints on spectral efficiency, channel coding must be done without an increase in the bandwidth. There is however an inherent tradeoff between code rate and CPM parameters. For instance, if a lower rate code is used, then in order to maintain a specified bandwidth efficiency, the modulation must have either a smaller modulation index, use wider pulse shapes, or a smaller signal set. For any particular scenario, it is not clear if the coding gain due to using lower rate codes will offset the performance loss due to modulation which is further from being orthogonal or due to the additional inter symbol interference (ISI) caused by longer pulse shapes.

In this paper, we attempt in part to address the ques-

tion put forth in [7]: “Which is the optimal combination of coding and CPM for a given bandwidth efficiency and detector complexity?” Considering all possible CPM pulse shapes and receiver designs would render a prohibitively large search space. Hence, we restrict our search to $\{2, 4\}$ -Gaussian frequency shift keying (GFSK), in fading channels. Due to its benefits outlined earlier, bit-interleaved coded GFSK is considered. The coherent detectors used in [2], [3], [7] are limited by complexity and susceptibility to phase estimation errors. We hence use the noncoherent (differential) soft-decision differential phase detector (SDDPD) [9] which with sequence detection, was shown to outperform [10] some popular differential detectors such as the limiter discriminator integrator [11] and the differential phase detector [12]. Different from [9] and [10] where the SDDPD with Viterbi decoding gives hard estimates on the modulated symbols, we develop a soft-out SDDPD (SO-SDDPD) that generates bit-wise log-likelihood ratios (LLRs) for the modulated symbols.

The Shannon capacity is the natural benchmark for BICM, since it is now possible to signal within 1 dB of the blocklength-constrained capacity using “off-the-shelf” capacity-approaching binary codes [13]. In this paper, we outline a method for determining the Shannon capacity under BICPM constraints. For our proposed system, we use the constrained capacity as a metric to drive the search for the most energy efficient combination of GFSK parameters and code rate over a wide range of spectral efficiencies. Our approach hence differs from the traditional methods of selecting

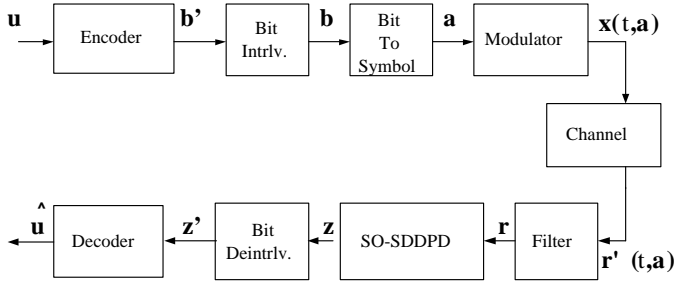


Fig. 1. System model.

CPM parameters based on maximizing Euclidian distance [2], [3], [5], [14]. The key benefit of a capacity based selection of CPM parameters is that it explicitly takes into account the tradeoff between code rate and modulation parameters, which is fundamental to the considered problem. Such an approach (to the best of our knowledge) has not been previously proposed.

BICM performance could be improved by feeding soft information back from the decoder to the demodulator, a process termed *BICM with iterative decoding* (BICM-ID) [15], [16] and has been applied to the BICPM paradigm in [6], [7]. We did simulate BICM-ID for our system, but for the range of parameters considered in this paper, there were no significant improvements over BICM. Hence a discussion on BICM-ID has been omitted from this paper.

II. SYSTEM MODEL

The system model is shown in Fig. 1.

A. Transmitter and Channel

A vector $\mathbf{u} \in \{0, 1\}^{N_u}$ of message bits is passed through the binary encoder to produce a codeword $\mathbf{b}' \in \{0, 1\}^{N_b}$. \mathbf{b}' is multiplied by a permutation matrix

$\mathbf{\Pi}$ to produce the bit-interleaved codeword $\mathbf{b} = \mathbf{b}'\mathbf{\Pi}$. \mathbf{b} is arranged in a $\log_2 M \times N_a$ matrix B such that, the matrix element $B_{i,k} = b_{k \log_2 M + i}$. Each column of B is mapped to one of M symbols (natural mapping) to produce the symbol sequence $\mathbf{a} \in \{\pm 1, \pm 3, \dots, \pm(M-1)\}^{N_a}$, where, $N_a = \lceil N_b / \log_2 M \rceil$. The M -ary, base-band GFSK signal in the interval $kT \leq t \leq (k+1)T$ is

$$x(t, \mathbf{a}) = \sqrt{P_x} \exp(\sqrt{-1} \varphi(t, \mathbf{a})), \quad (1)$$

where $P_x = \mathcal{E}_s / 2T$ with symbol energy \mathcal{E}_s and symbol period T . The phase of the GFSK signal can be written as [12]

$$\varphi(t, \mathbf{a}) = \pi h \sum_{i=-\infty}^{\infty} a_i \int_{-\infty}^t g(\tau - iT) d\tau, \quad (2)$$

where h is the modulation index, and $g(\tau)$ is the response of the Gaussian shaping filter to a rectangular pulse of duration T . In particular for GFSK,

$$g(t) = [Q(-cB_g t) - Q(-cB_g(t - T))] / T, \quad (3)$$

where $c = 7.546$ and $B_g T$ is the normalized 3 dB bandwidth of the filter. The Q function is given by $Q(x) = (2\pi)^{-1/2} \int_x^{\infty} \exp(-y^2/2) dy$.

The GFSK modulated signal at the output of a frequency nonselective, Rician channel is

$$r'(t, \mathbf{a}) = c(t)x(t, \mathbf{a}) + n'(t), \quad (4)$$

where,

$$c(t) = \sqrt{P_s} + \sqrt{P_d} \xi(t). \quad (5)$$

P_s is the power gain of the direct signal component, P_d is the power gain of the diffused component, and the Rician K -factor is given by $K = P_s / P_d$. P_s and P_d are

normalized such that $P_s + P_d = 1$. When $K = 0$, the channel is Rayleigh and when $K = \infty$, the channel is AWGN. $\xi(t)$ is a zero mean, complex Gaussian fading process with variance $1/2$ in each complex dimension. Lastly, $n'(t)$ is additive, zero-mean, complex white Gaussian noise with power spectral density $N_o/2$.

B. Receiver

The received signal r' is passed through a front-end receive filter that removes the out-of-band noise. The filter noise bandwidth (B_n) is assumed to be greater than the signal's 99% power bandwidth, hence the signal remains sufficiently undistorted by the filter. The signal at the output of the filter is

$$r(t, \mathbf{a}) = c(t)x(t, \mathbf{a}) + n(t), \quad (6)$$

where, $n(t)$ is bandlimited Gaussian noise. The phase of the filtered signal can be written as

$$\phi(t, \mathbf{a}) = \varphi(t, \mathbf{a}) + \eta(t), \quad (7)$$

where the phase noise $\eta(t)$ is as defined in [12].

The SO-SDDPD finds the phase difference between successive symbol intervals. The received phase differences are used to produce bit-wise LLRs \mathbf{z} , which are deinterleaved (\mathbf{z}') and passed to the input of a channel decoder. The decoder uses \mathbf{z}' in its local/internal iterations (assuming the decoder is iterative) and generates estimates of the data bits, denoted as $\hat{\mathbf{u}}$.

III. SO-SDDPD

The SO-SDDPD finds the phase difference between successive symbol intervals as

$$\Delta\phi_k = (\Delta\varphi_k + \eta(t_k, \mathbf{a}) - \eta(t_k - T, \mathbf{a})) \mod 2\pi, \quad (8)$$

for $k = 0, 1, \dots, N_a - 1$. Assuming the GFSK induced ISI extends up to Z symbols [12],

$$\Delta\varphi_k = \pi h \sum_{i=-(Z-1)}^{(Z-1)} a_{k-i} \int_{iT+T}^{iT} g(t) dt. \quad (9)$$

From (9), it is seen that $\Delta\varphi_k$ will assume one of M^{Z+1} values. The phase region between $0-2\pi$ is divided into R sub-regions. The detector finds one of the R possible sub-regions (D_k), in which $\Delta\phi_k$ lies. The sequence of sub-regions $\mathbf{D} = (D_0, D_1, \dots, D_{N_a-1})$ is then sent to a branch metric calculator. Let $\Delta\varphi^i = (\Delta\varphi_0^i, \Delta\varphi_1^i, \dots, \Delta\varphi_{N_a-1}^i)$ be the phase differences corresponding to any transmitted sequence $\mathbf{a}^i = (a_{-1}^i, a_0^i, a_1^i, \dots, a_{N_a-1}^i)$, where a_{-1}^i is used to initialize the detector trellis. The branch metric calculator finds the conditional probabilities of receiving \mathbf{D} , given $\Delta\varphi^i$ i.e. $P(\mathbf{D}|\Delta\varphi^i)$. The metric for the i^{th} path in the trellis at a symbol interval k is [9]

$$\begin{aligned} P(D_k|\Delta\varphi_k^i) &= P(\varrho_k^1 \leq \Delta\varphi_k^i < \varrho_k^2) \\ &= 1 + F(\varrho_k^2|\Delta\varphi_k^i) - F(\varrho_k^1|\Delta\varphi_k^i), \varrho_k^1 \leq \Delta\varphi_k^i < \varrho_k^2 \\ &= F(\varrho_k^2|\Delta\varphi_k^i) - F(\varrho_k^1|\Delta\varphi_k^i), \text{otherwise.} \end{aligned} \quad (10)$$

ϱ_k^1 and ϱ_k^2 are the boundaries of the sub-region D_k . The branch metrics are precalculated and stored in a $M^{Z+1} \times R$ look up table. The nonlinear function F for M -GFSK can be derived from [12].

The SO-SDDPD estimates the LLR for $B_{i,k}$ as

$$\mathcal{Z}_{i,k} = \log \frac{\sum_{\mathcal{B}^{(1)}} \alpha_{k-1}(s') \gamma_k(s', s) \beta_k(s)}{\sum_{\mathcal{B}^{(0)}} \alpha_{k-1}(s') \gamma_k(s', s) \beta_k(s)}, \quad (11)$$

where, α , β and γ are the metrics in the BCJR algorithm. $\mathcal{B}^{(1)}$ is the set of state transitions $\{S_{k-1} =$

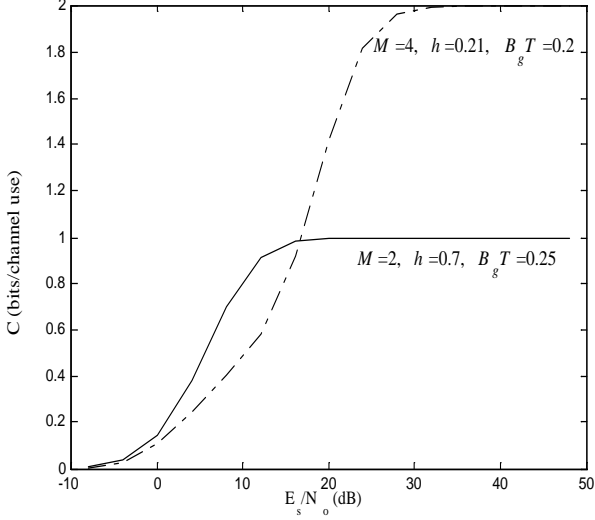


Fig. 2. BICPM capacity of 2-GFSK ($h = 0.7$, $B_g T = 0.25$) and 4-GFSK ($h = 0.21$, $B_g T = 0.2$) in a Rayleigh channel, under the constraint of using SO-SDDPD. The SO-SDDPD uses $R = 40$ uniform phase regions for 2-GFSK and $R = 26$ uniform phase regions for 4-GFSK.

$s'\} \rightarrow \{S_k = s\}$ corresponding to $B_{i,k} = +1$ and $\mathcal{B}^{(0)}$ is defined similarly for $B_{i,k} = 0$. The branch metric is

$$\gamma_k(s', s) = P(D_k | \Delta\varphi_k).$$

The LLRs in the matrix \mathcal{Z} can be arranged into a vector \mathbf{z} such that, $z_{k \log_2 M + i} = \mathcal{Z}_{i,k}$. The deinterleaved LLRs from the demodulator (\mathbf{z}') is fed to the channel decoder, which after performing a certain number of iterations, forms estimates of the data bits $\hat{\mathbf{u}}$.

IV. CAPACITY UNDER BICPM CONSTRAINTS

The mutual information between a channel input x' and output y' is defined as [18]

$$I(x', y') = \int \int p(x', y') \log_2 \frac{p(x', y')}{p(x')p(y')} dx' dy'. \quad (12)$$

The channel capacity is simply the mutual information maximized over all possible input distributions

$$C = \max_{p(x')} I(x', y'). \quad (13)$$

However, in a practical system, the input distribution is constrained by the choice of the modulation parameters. The capacity is hence the mutual information between the bit at the modulator input and the LLR at the demodulator output. Additionally, BICM transforms the channel into $\log_2 M$ parallel channels such that the capacity of the i^{th} channel in nats is [8]

$$C_i = E_{a,n,c,s' \rightarrow s} [\log(2) + \log p(b_i | \mathbf{r})]. \quad (14)$$

E denotes the expectation operation, which is performed over all possible symbols a , fading coefficient c , noise n and state transitions $s' \rightarrow s$. It is assumed that the fading coefficient $c(t) = c$ remains fixed over the duration of a state transition $s' \rightarrow s$. Further, since the trellis sections are identical, the subscript denoting symbol intervals can be dropped from the equations. The above equation can also be written as

$$\begin{aligned} C_i &= \log(2) + E_{a,c,n,s' \rightarrow s} \left[\log \frac{p(b_i | \mathbf{r})}{p(b_i=0|\mathbf{r}) + p(b_i=1|\mathbf{r})} \right] \\ &= \log(2) - E_{a,c,n,s' \rightarrow s} \left[\log \frac{p(b_i=0|\mathbf{r}) + p(b_i=1|\mathbf{r})}{p(b_i | \mathbf{r})} \right] \\ &= \log(2) - E_{a,c,n,s' \rightarrow s} \left[\log \left\{ \exp \log \frac{p(b_i=0|\mathbf{r})}{p(b_i | \mathbf{r})} + \exp \log \frac{p(b_i=1|\mathbf{r})}{p(b_i | \mathbf{r})} \right\} \right]. \quad (15) \end{aligned}$$

Since the \max^* operator can also be written as [19]

$$\begin{aligned} \max^* \{x, y\} &= \max(x, y) + \log \{1 + \exp\{-|y - x|\}\} \\ C_i &= \log(2) - E_{a,c,n,s' \rightarrow s} \left[\max^* \left\{ \log \frac{p(b_i=0|\mathbf{r})}{p(b_i | \mathbf{r})}, \log \frac{p(b_i=1|\mathbf{r})}{p(b_i | \mathbf{r})} \right\} \right]. \quad (16) \end{aligned}$$

Now assigning $y = \log \frac{p(b_i=1|\mathbf{r})}{p(b_i|\mathbf{r})}$ and $x = \log \frac{p(b_i=0|\mathbf{r})}{p(b_i|\mathbf{r})}$

C_i can be written as

$$C_i = \log(2) - E_{a,c,n,s' \rightarrow s} [\max(x, y) + \log \{1 + \exp\{-|y - x|\}\}]. \quad (17)$$

The above equation can also be expressed as

$$C_i = \log(2) - E_{a,c,n,s' \rightarrow s} [\max * \{0, z_i(-1)^{b_i}\}].$$

Since the capacities of parallel channels add, the BICPM capacity is simply

$$\begin{aligned} C &= \sum_{i=1}^{\log_2 M} C_i \\ &= \sum_{i=1}^{\log_2 M} \log(2) - E_{a,c,n,s' \rightarrow s} [\max * \{0, z_i(-1)^{b_i}\}]. \end{aligned}$$

The ergodic BICPM capacity when converted to bits per channel use of our system is now

$$C = \log_2 M - \frac{1}{\log(2)} \sum_{i=1}^{\log_2 M} E_{a,c,n,s' \rightarrow s} [\max * \{0, z_i(-1)^{b_i}\}]. \quad (18)$$

Since a convenient closed form integral does not exist, (18) is found using Monte Carlo simulations. Since the soft-outputs \mathbf{z} are influenced by R and Z , the capacity is also constrained by the detector design. Fig. 2 shows the constrained BICPM capacity versus \mathcal{E}_s/N_o for 2-GFSK ($h = 0.7$, $B_g T = 0.25$) and 4-GFSK ($h = 0.21$, $B_g T = 0.2$) in Rayleigh fading, using SO-SDDPD with $R = 40$ and $R = 26$ respectively. The information theoretic minimum \mathcal{E}_s/N_o ($\min\{\mathcal{E}_s/N_o\}$) at code rate R_c is found by reading (from a figure similar to Fig. 2, with the appropriate GFSK parameters) the value of \mathcal{E}_s/N_o for $C = R_c \log_2 M$. The information theoretic minimum \mathcal{E}_b/N_o ($\min\{\mathcal{E}_b/N_o\}$) to achieve an

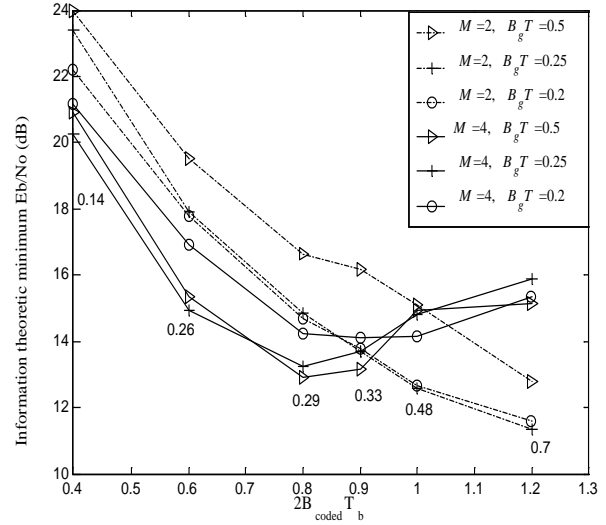


Fig. 3. Information theoretic minimum \mathcal{E}_b/N_o ($\min\{\mathcal{E}_b/N_o\}$) in dB at different $2B_{coded}T_b$ for a rate 5/6 coded $\{2, 4\}$ -GFSK, with SO-SDDPD based BICPM, in Rayleigh fading. The numbers denote modulation indices corresponding to GFSK parameters with the lowest $\min\{\mathcal{E}_b/N_o\}$ at different $2B_{coded}T_b$.

arbitrary low BER at a given R_c is now $\min\{\mathcal{E}_b/N_o\} = \min\{\mathcal{E}_s/N_o\}/R_c \log_2 M$, since $\mathcal{E}_s = \mathcal{E}_b R_c \log_2 M$.

V. CAPACITY BASED SELECTION OF GFSK PARAMETERS

The parameters of interest, viz, R_c , M , h and $B_g T$ can take on a wide range of values. Practical considerations dictate that the selection of GFSK parameters and code rates at different spectral efficiencies must be done under some constraints. In this paper, we limit ourselves to code rates $R_c \in \{6/7, 5/6, 3/4, 2/3, 1/2, 1/3, 1/4, 1/5\}$. The spectral efficiency is measured by the normalized double-sided 99% coded bandwidths ($2B_{coded}T_b$) (T_b is the bit period). We constrain the search to the representative set, $2B_{coded}T_b \in \{0.4, 0.6, 0.8, 0.9, 1.0, 1.2\}$. $\{2, 4\}$ -GFSK

are considered, and to limit complexity the detector always assumes $Z = 2$. Unless specified otherwise, SO-SDDPD uses uniformly spaced phase sub-regions such that $R = 40$ for $M = 2$ and $R = 26$ for $M = 4$, also \mathbf{z} are generated using the log-MAP algorithm [19]. Similar to [12], $B_gT = 0.5, 0.25$ and 0.2 are considered.

Using the signal power spectral densities, at each R_c , the value of h is found that meets the required $2B_{coded}T_b$ for each value of B_gT and M . This is done using the relationship between R_c and uncoded power spectral density from [3]. Using (18), $\min\{\mathcal{E}_b/N_o\}$ is found for all allowable combinations of M , h , B_gT and R_c at each $2B_{coded}T_b$. Fig. 3 shows $\min\{\mathcal{E}_b/N_o\}$ versus $2B_{coded}T_b$ when $R_c = 5/6$. At each $2B_{coded}T_b$, there are 6 combinations of M , h and B_gT (due to our search constraints), out of which the GFSK parameters yielding the lowest $\min\{\mathcal{E}_b/N_o\}$ are selected. Since it is not feasible to list the 36 different values of h , only those values corresponding to the lowest $\min\{\mathcal{E}_b/N_o\}$ at each spectral efficiency are listed in Fig. 3. As an example for $2B_{coded}T_b = 1.2$, $M = 2$, $h = 0.7$, $B_gT = 0.25$ has the lowest $\min\{\mathcal{E}_b/N_o\}$ with $R_c = 5/6$.

For a given B_gT , as the spectral efficiency decreases, the allowable value of h increases. Typically (but not necessarily), larger values of h result in lower values of $\min\{\mathcal{E}_b/N_o\}$. Since by lowering B_gT , we can have a larger value of h for the same $2B_{coded}T_b$, it may be possible to reduce $\min\{\mathcal{E}_b/N_o\}$ by selecting smaller values of B_gT . However, reducing B_gT increases the GFSK induced ISI, whereas our detector accounts only

for adjacent symbol interference ($Z = 2$). Hence, when B_gT is lowered beyond a certain value, the benefits of an increased h may be offset by unaccounted GFSK induced ISI at the receiver as is evident from Fig. 3.

A similar search was conducted for all listed values of R_c . This gives us the set of M , h and B_gT with the lowest $\min\{\mathcal{E}_b/N_o\}$ at different $2B_{coded}T_b$ for each of the considered code rates. The search is further narrowed to find the combination of R_c and GFSK parameters that have the lowest $\min\{\mathcal{E}_b/N_o\}$ for a particular spectral efficiency. This is illustrated in Fig. 4 for $2B_{coded}T_b = 0.8$. Shown here is the lowest $\min\{\mathcal{E}_b/N_o\}$ for each of the different R_c . For our proposed system, it is apparent that $R_c = 3/4$ with $M = 4$, $h = 0.25$ and $B_gT = 0.5$ has the best energy efficiency at $2B_{coded}T_b = 0.8$. Fig. 4 also illustrates the tradeoff between between code rate and GFSK parameters at a fixed bandwidth efficiency. As R_c is lowered from $6/7$ to $3/4$, improvement in the energy efficiency is seen. However, when R_c is lowered below $3/4$, the scaling of GFSK parameters (primarily h) not only offsets any potential coding gain, but in fact worsens the performance by increasing the $\min\{\mathcal{E}_b/N_o\}$. The combination of GFSK parameters and code rates with the lowest $\min\{\mathcal{E}_b/N_o\}$ at the different spectral efficiencies is listed in Table I for a Rayleigh channel and in Table II for a Rician channel ($K = 6$ dB). It is observed that for the considered BICPM system, 4-GFSK outperforms 2-GFSK except at the worst considered spectral efficiency. It is observed that with increasing K , the best code rate tends

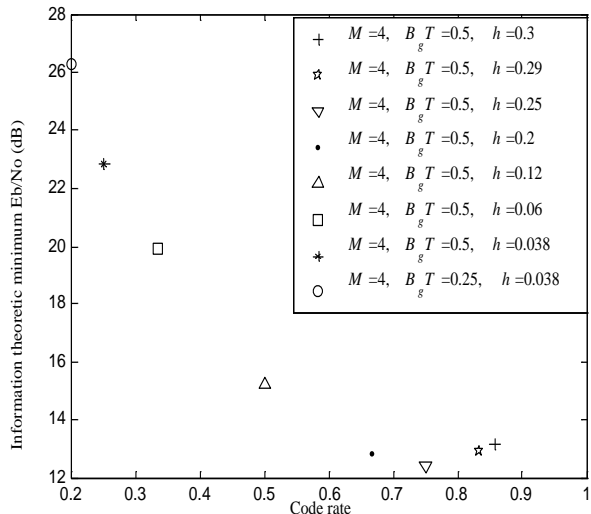


Fig. 4. GFSK parameters with the lowest information theoretic minimum \mathcal{E}_b/N_o (dB) for various code rates at $2B_{coded}T_b = 0.8$ in Rayleigh fading. At $2B_{coded}T_b = 0.8$, it is seen that $R_c = 3/4$ with $M = 4$, $h = 0.25$ and $B_gT = 0.5$ has the best energy efficiency for BICPM with SO-SDDPD.

to increase for each value of $2B_{coded}T_b$.

VI. ERROR RATE SIMULATIONS

Bit error rate (BER) simulations were performed for the proposed BICPM system using the UMTS turbo code [20] to demonstrate the utility of the constrained capacity as a performance measure. Codeword length of $N_b = 6720$ bits was used. While the mother code rate is $R_c = 1/3$, rate matching was performed to obtain higher code rates. At every \mathcal{E}_b/N_o , at least 30 frame errors were logged.

The BER after 16 turbo decoder iterations for our proposed BICPM system with 4-GFSK ($h = 0.24$, $B_gT = 0.5$) in Rayleigh fading is shown in Fig. 5 (solid curve). Here, a rate $2/3$ turbo code was used, which for the considered GFSK parameters gives

TABLE I
COMBINATION OF CODE RATES AND GFSK PARAMETERS WITH
LOWEST INFORMATION THEORETIC MINIMUM \mathcal{E}_b/N_o UNDER
THE CONSTRAINT OF USING SO-SDDPD IN RAYLEIGH FADING
AT DIFFERENT $2B_{coded}T_b$.

$2B_{coded}T_b$	Rate	M	B_gT	h	$\min\{\mathcal{E}_b/N_o\}$ dB
0.4	3/4	4	0.2	0.195	18.15 dB
0.6	2/3	4	0.2	0.21	18.08 dB
0.8	3/4	4	0.5	0.25	12.38 dB
0.9	2/3	4	0.5	0.24	11.99 dB
1.0	2/3	4	0.5	0.3	11.44 dB
1.2	5/6	2	0.25	0.7	11.34 dB

$2B_{coded}T_b = 0.9$. The simulated \mathcal{E}_b/N_o required to achieve an arbitrarily low BER (assumed 10^{-5}) is found from Fig. 5 to be 12.93 dB. This combination of code rate and GFSK parameters gives $2B_{coded}T_b = 0.9$ and $\min\{\mathcal{E}_b/N_o\} = 11.99$ dB (Table I). The simulation results reveal that it is indeed possible to signal within 1 dB of the information theoretic limit by simply using an off-the-shelf binary turbo code.

While signalling at specific spectral efficiencies, performance comparisons between coded and uncoded systems must be made at the same bandwidth efficiency. Fig. 5 shows the BER comparison between our proposed BICPM system and an uncoded system, also detected using the SO-SDDPD. The parameters for uncoded GFSK are $M = 2$, $h = 0.5$ and $B_gT = 0.3$ which gives $2B_{uncoded}T_b = 0.9$ (incidentally these values of M , h and B_gT are used in the GSM specifications). A coding gain of 16 dB is observed at $\text{BER} = 10^{-5}$.

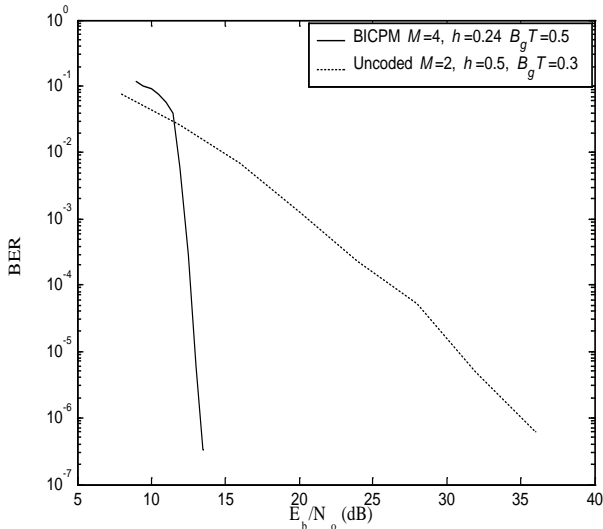


Fig. 5. BER for SO-SDDPD ($R = 26$) based BICPM using a rate $2/3$ turbo code in Rayleigh fading. Shown is the BER after 16 decoder iterations. The coded GFSK parameters $M = 4$, $h = 0.24$ and $B_g T = 0.5$ with $R_c = 2/3$ give $2B_{coded}T_b = 0.9$. Also shown is the BER for uncoded, SO-SDDPD ($R = 40$) detected GFSK. The uncoded GFSK parameters $M = 2$, $h = 0.5$ and $B_g T = 0.3$ give $2B_{uncoded}T_b = 0.9$.

VII. CONCLUSION

The Shannon capacity of bit-interleaved coded CPM under modulation, channel, and detector constraints is a very practical predictor of system performance due to the availability of off-the-shelf capacity-approaching binary codes. Since most CPM systems and their associated demodulators are too complex to admit a closed-form solution, a method for determining the constrained capacity using Monte Carlo integration has been proposed. A soft-out, soft-decision differential phase detector has been developed for noncoherent detection of GFSK signals. For a select range of code rates, spectral efficiencies and GFSK parameters, the BICM capacity under modulation and SO-SDDPD

TABLE II
COMBINATION OF CODE RATES AND GFSK PARAMETERS WITH
LOWEST INFORMATION THEORETIC MINIMUM \mathcal{E}_b/N_o UNDER
THE CONSTRAINT OF USING SO-SDDPD IN RICIAN FADING
($K = 6$ dB) AT DIFFERENT $2B_{coded}T_b$.

$2B_{coded}T_b$	Rate	M	$B_g T$	h	$\min\{\mathcal{E}_b/N_o\}$ dB
0.4	3/4	4	0.2	0.195	15.38 dB
0.6	5/6	4	0.5	0.18	11.67 dB
0.8	5/6	4	0.5	0.29	9.09 dB
0.9	3/4	4	0.5	0.285	8.87 dB
1.0	2/3	4	0.5	0.3	8.83 dB
1.2	6/7	2	0.25	0.76	8.39 dB

design constraints has been calculated in Rayleigh and Rician fading. This constrained capacity is used to identify the combination of GFSK parameters and code rates with the best energy efficiency for a desired spectral efficiency.

Due to the large number of variables involved, we had to limit the search space. Even under these constraints, 576 different capacity calculations were required to generate the two final tables. An extension of this work could be to consider $M > 4$, more values of $B_g T$, code rates, bandwidth efficiencies and receiver architectures (such as coherent receivers or SO-SDDPD with $Z > 2$). Since the search space is so large, a more efficient way to go through the search space could be to use a gradient algorithm or even an evolutionary algorithm.

REFERENCES

- [1] J. B. Anderson, T. Aulin, and C. E. Sundberg, *Digital Phase Modulation*. New York: Plenum Press, 1986.

- [2] S. V. Pizzi and S. G. Wilson, "Convolutional coding combined with continuous phase modulation," *IEEE Trans. Commun.*, vol. 33, pp. 20–29, Jan. 1985.
- [3] T. Svensson and A. Svensson, "On convolutionally encoded partial response CPM," in *Proc. IEEE Vehicular Tech. Conf.*, (Amsterdam), pp. 663–667, Sept. 1999.
- [4] R. W. Kerr and P. J. McLane, "Coherent detection of interleaved trellis encoded CPFSK on shadowed mobile satellite channels," *IEEE Trans. Veh. Tech.*, vol. 41, pp. 159 – 169, May. 1992.
- [5] L. Yiin and G. L. Stüber, "Noncoherently detected trellis-coded partial response CPM on mobile radio channels," *IEEE Trans. Commun.*, vol. 44, pp. 967–975, Aug. 1996.
- [6] K. R. Narayanan and G. L. Stüber, "Performance of trellis-coded CPM with iterative demodulation and decoding," *IEEE Trans. Commun.*, vol. 49, pp. 676–687, Apr. 2001.
- [7] P. Moqvist and T. Aulin, "Serially concatenated continuous phase modulation with iterative decoding," *IEEE Trans. Commun.*, vol. 49, pp. 1901–1915, Nov. 2001.
- [8] G. Caire, G. Taricco, and E. Biglieri, "Bit-interleaved coded modulation," *IEEE Trans. Inform. Theory*, vol. 44, pp. 927–946, May. 1998.
- [9] J. P. Fonseka, "Soft-decision differential phase detection with Viterbi decoding in satellite mobile systems," *Jrnl. of Commun. and Netw.*, pp. 265–272, Sept. 2001.
- [10] R. I. Seshadri, D. Lao, C. Kwan, and J. P. Fonseka, "Bandwidth constrained, low complexity noncoherent CPM with ML soft-decision differential phase detection," in *Proc. IEEE MILCOM Conference*, (Atlantic City, NJ), Oct. 2005.
- [11] I. Korn, "GMSK with limiter discriminator integrator detection in satellite mobile channel," *IEE Proc. Commun.*, vol. 136, pp. 361–366, Oct. 1989.
- [12] I. Korn, "GMSK with differential phase detection in the satellite mobile channel," *IEEE Trans. Commun.*, vol. 38, pp. 1980–1986, Nov. 1990.
- [13] S. Dolinar, D. Divsalar, and F. Pollara, "Turbo code performance as a function of code block size," in *Proc. Int. Symp. on Information Theory*, (Boston), Aug. 1998.
- [14] P. Moqvist and T. Aulin, "Power and bandwidth efficient serially concatenated CPM with iterative decoding," in *Proc. IEEE GLOBECOM Conference*, vol. 2, (San Francisco, CA), pp. 790 – 794, Nov. 2000.
- [15] X. Li and J. A. Ritcey, "Bit-interleaved coded modulation with iterative decoding," *IEEE Commun. Letters*, vol. 1, pp. 169–171, Nov. 1997.
- [16] M. C. Valenti and S. Cheng, "Iterative demodulation and decoding of turbo coded M-ary noncoherent orthogonal modulation," *IEEE Journ. on Selec. Areas. of Commun.*, vol. 23, pp. 1739 – 1747, Sep. 2005.
- [17] L. Bahl, J. Cocke, F. Jelinek, and J. Raviv, "Optimal decoding of linear codes for minimizing symbol error rate," *IEEE Trans. Inform. Theory*, vol. 20, pp. 284–287, Mar. 1974.
- [18] T. Cover and J. Thomas, *Elements of Information Theory*. New York: Wiley Interscience, 1991.
- [19] A. Viterbi, "An intuitive justification and a simplified implementation of the MAP decoder for convolutional codes," *IEEE Journ. on Selec. Areas. of Commun.*, vol. 16, pp. 260–264, Feb. 1998.
- [20] European Telecommunications Standard Institute, Universal mobile telecommunications system, "Multiplexing and channel coding (FDD)," *3GPP2 TS 125.212 Version 6.6.0*, Sep. 2005.